# Multiple-scale adjoint sensitivity analysis of hydrodynamic/thermo-acoustic instability in turbulent combustion chambers

**By L. Magri†, Y. C. See, M. Ihme AND M. P. Juniper†**

In this paper, we define a mathematically consistent set of thermo-acoustic equations via asymptotic multiple scale methods in the low-Mach number limit. The final thermo-acoustic equations consist of reacting low-Mach number (LMN) equations for hydrodynamic phenomena and acoustic (AC) equations. The two sets of equations are two-way coupled. The coupling terms depend on which multiple scales are used. We derive and discuss the coupling terms for three distinct limits: double-time-double-space (2T-2S); double-time-single-space (2T-1S); and single-time-double-space (1T-2S). We linearize the thermo-acoustic equations around the mean flow, which is obtained by time averaging Large-Eddy simulations. We show that only 1T-2S provides a two-way coupled linearized system. In the other limits, the coupling from the AC to the LMN is of higher order. We perform global direct and adjoint analysis to identify unstable modes and passive-feedback mechanisms to stabilize/lower the frequency of the oscillation. Preliminary results are shown for a dual-swirl gas turbine combustor and a simplified dump combustor.

## 1. Introduction

Thermo-acoustic oscillations occur in gas turbine and rocket engines. They can lead to catastrophic failure and are one of the most persistent problems in gas turbines and rocket engines. If acoustic pressure fluctuations occur in phase with heat release fluctuations then thermal energy is converted to mechanical energy over a cycle and the acoustic amplitude increases. If the fluctuating heat arises from a flame then these fluctuations depend on coherent periodic structures that convect and grow down the flame. These structures are driven by shear and centrifugal forces and do not necessarily travel at the speed of the mean flow. Experiments show that the interaction between the hydrodynamic and thermo-acoustic mechanisms determines the overall thermo-acoustic behavior of the flow in configurations in which the flame sits in a region that is strongly hydrodynamically unstable (Chakravarthy *et al.* 2007). The gas turbine model combustor by Meier and co-workers (Giezendanner *et al.* 2005; Allison *et al.* 2013) is an example of such a configuration. This burner has been designed to model those in gas turbines so it is likely that the same features will be found in industrial applications. The aim of the techniques developed in this study is to identify the mechanisms of coupled instability, the regions of the flow that cause the instability, and strategies for reducing the growth rates of the instability. This project involves the multiphysical interaction of hydrodynamic and thermo-acoustic instability mechanisms, modelled in a multiple time/space scale perturbation framework (Balaji 2012).

† Department of Engineering, University of Cambridge, UK

## 2. Governing equations

The compressible continuity, momentum and energy equations, in which $S_1$ is the oxidizer-to-fuel density ratio, are

$$\frac{\partial \rho}{\partial \tau} + \left(\frac{L}{h}M\right) \nabla \cdot (\rho \mathbf{u}) = 0, \tag{2.1}$$

$$\rho \frac{\partial \mathbf{u}}{\partial \tau} + \left(\frac{L}{h}M\right) \left[\rho \mathbf{u} \cdot \nabla \mathbf{u} + \frac{1}{\gamma M^2}\nabla p - \frac{1}{S_1 Re}\nabla \cdot \boldsymbol{\tau}\right] = 0, \tag{2.2}$$

$$\rho \frac{\partial T}{\partial \tau} + \left(\frac{L}{h}M\right) \left[\rho \mathbf{u} \cdot \nabla T - \frac{1}{S_1 RePr}\Delta T - \rho Da Q_R\right] + \dots$$

$$\dots \frac{\gamma - 1}{\gamma}\left(\frac{\partial p}{\partial \tau} + \frac{ML}{h}\mathbf{u} \cdot \nabla p\right) + \frac{L}{h} o\left(M\right) = 0. \tag{2.3}$$

The reference length is the mean flame length, $h$, upstream of which 90% of the total heat release occurs. The reference time is $L/\tilde{c}_0$, where $\tilde{c}_0$ is the reference speed of sound and $L$ the combustor's length (Figure 1). $\tau$ is the dimensionless time. We have neglected body forces and assumed Stokes' constitutive law, $\boldsymbol{\tau} = \nabla \mathbf{u} + \nabla^T \mathbf{u} - 2/3\left(\nabla \cdot \mathbf{u}\right)\mathbf{I}$, and Fourier law for conduction. Thermal conductivity, heat capacities and viscosity are constant. The gas is perfect. In the energy equation, we assume that variations in the pressure, $p$, are negligible from now on. This is a common assumption in subsonic high-Reynolds number combustion problems. We neglect viscous dissipation and variations in the kinetic energy, which are $\sim o(M)$ in Eq. (2.3). (The little-$o$ notation is such that $\lim_{M\to 0} o(M)/M = 0$.)

We study diffusion flames with one-step chemistry by defining the mixture fraction, $Z$, and using the non-dimensional Arrhenius' law (Nichols & Schmid 2008)

$$\rho \frac{\partial Z}{\partial \tau} + \left(\frac{L}{h}M\right) \left[\rho \mathbf{u} \cdot \nabla Z - \frac{1}{S_1 ReSc}\Delta Z\right] = 0, \tag{2.4}$$

$$Q_R = \rho^2 \omega = \rho^2 \left[\left(Z - \frac{T}{s+1}\right)\left(1 - Z - \frac{sT}{s+1}\right) - \kappa T^2\right] \exp\left[\frac{-\beta\left(1-T\right)}{1 - \alpha\left(1-T\right)}\right], \tag{2.5}$$

where $Sc$ is the Schmidt number; $s$ is the equilibrium constant; $\kappa$ is the heat-release parameter; $\alpha$ is a negative number depending on the flame temperature; $\beta$ is the Zeldovich number; and the Lewis number is assumed to be unity. The state equation becomes

$$\rho\left[\left(S_1 - 1\right)Z + 1\right]\left[\left(S_2 - 1\right)T + 1\right] - p = 0, \tag{2.6}$$

where $S_1$ is the oxidizer-to-fuel density ratio and $S_2$ is the adiabatic-flame-to-ambient temperature ratio.

## 3. Two-way coupling of hydrodynamic processes with acoustics

In this section, we couple the reacting low-Mach Number (LMN) equations with the acoustic (AC) equations in a mathematically consistent manner by combining an asymptotic approach with a multiple-scale method. This enables us to reduce the complexity of the full problem governed by Eqs. (2.1)-(2.6). The literature about multiple-scale methods is comprehensive (Zeytounian 2006). In thermo-acoustics, multiple-scale methods were applied, among others, by Mariappan & Sujith (2011) and Balaji (2012).

Processes governed by the reacting LMN equations will be referred as to hydrodynamic. In our problems, the two perturbation parameters are the Mach number, $M \sim O(\epsilon^1)$,

and the flame compactness, $h/L \sim O(\epsilon^n)$, where $h$ is the flame length, $L$ is the longitudinal combustor's length (Figure 1) and $\epsilon = o(1)$. The Mach number is the leading perturbation parameter, so $0 \leq n \leq 1$. In the combustion chambers under investigation, acoustic phenomena evolve at different scales to those of hydrodynamic phenomena. This is because low-frequency thermo-acoustic instabilities are expected to scale with the longitudinal length, $L$, whereas hydrodynamic instabilities are expected to scale with the flame length or shear-layer thickness, $h$. We define $t$ as the hydrodynamic time, $\tau$ as the acoustic time, $x_i$ as the hydrodynamic space, and $\xi_i$ as the acoustic space. Observing that hydrodynamic phenomena scale with the convective time, $h/\tilde{u}_0$, and flame length, $h$; and acoustic phenomena scale with the acoustic time, $L/\tilde{c}_0$, and combustor's length, $L$, it follows that

$$t/\tau = ML/h = \epsilon^{1-n}, \tag{3.1}$$

$$x_i/\xi_i = L/h = \epsilon^{-n}. \tag{3.2}$$

Physically, we need $\epsilon^{(n-1)} \geq 1$ AC time units, $\tau$, to get one convective time unit, $t$. In such a case the AC time is faster than the convective time. Likewise, we need $\epsilon^n \leq 1$ AC spatial units, $\xi_i$, to get one convective spatial unit, $x_i$. In such a case the AC space is longer than the convective space. We show and discuss three multiple-scale limits. First, the double-time-double-space limit (2T-2S), in which the acoustics evolve at shorter time scales and longer spatial scales than the hydrodynamics. The full description of this approach is given by Balaji (2012), who carried out nonlinear simulations of diffusion flames in a backward-facing step dump combustor. In this case $0 < n < 1$, i.e., the perturbation coefficient is strictly positive and smaller than unity. Second, the double-time-single-space limit (2T-1S), in which the acoustics evolve at shorter time scale but the same spatial scale as the hydrodynamics (Müller 1998). In this case $n = 0$, i.e., there are no different spatial scales. Third, the single-time-double-space limit (1T-2S), in which the acoustics evolve at longer spatial scale but same time scale as the hydrodynamics. In this case $n = 1$, i.e., there are no different time scales.

Klein (2005) used a 1T-2S multiple-scale method in non-reacting atmospheric flows. Mariappan & Sujith (2011) used a 1T-2S approach to model the Rijke-tube, in which the heat is released by an electrical wire. In their study, no flame equations were accounted for and the acoustics were one-dimensional. The effect that the acoustics has on the hydrodynamics was considered to be uniform in the hydrodynamic domain. We take these methods further and apply them to three-dimensional problems with flames.

### 3.1. *Asymptotic expansion and multiple scales*

In this section we outline the procedure applied to the original Eqs. (2.1)-(2.6) to reduce its complexity and separate out hydrodynamic and acoustic processes: (i) Asymptotic expansion. We expand the variables assuming a low-Mach number. This yields $\phi = \sum_i \epsilon^i \phi_i$, where the perturbation parameter is $\epsilon = \gamma^{\frac{1}{2}} M$ and $\phi$ denotes a generic variable. The heat capacity ratio is $\gamma \sim O(1)$, from which $\epsilon \sim O(M)$. (ii) Differential operator decomposition. In the double-time-double-space approach (2T-2S), $\phi(x,t) \rightarrow \phi(x,\xi,t,\tau)$. By applying the chain rule we decompose both the time and spatial derivatives: $\partial/\partial\tau \rightarrow \partial/\partial\tau + \epsilon^{1-n}\partial/\partial t$; $\nabla \rightarrow \nabla^x + \epsilon^n \nabla^\xi$. In the double-time-single-space approach (2T-1S), $\phi(x,t) \rightarrow \phi(x,t,\tau)$. Here, we decompose only the time derivative as $\partial/\partial\tau \rightarrow \partial/\partial\tau + \epsilon^{1-n}\partial/\partial t$. In the single-time-double-space approach (1T-2S), $\phi(x,t) \rightarrow \phi(x,\xi,t)$. Here, we decompose only the spatial derivative as $\nabla \rightarrow \nabla^x + \epsilon^n \nabla^\xi$. (iii) Order-by-order matching. New equations are defined order by order in $\epsilon$. (iv) Average-plus-

fluctuation decomposition and equation averaging. In 2T-2S, the time decomposition $\phi = \langle\phi\rangle_\tau + \phi^{'\tau}$ is substituted into the operator presented in (ii) and the equations are temporally averaged over the slow LMN time scale $t$. $\langle\cdot,\cdot\rangle_\tau$ represents the time average of the fast variable $\tau$, the superscript $^{'\tau}$ represents the fluctuation over the fast time $\tau$. Then the variables are split up as $\phi = \langle\phi\rangle_x + \phi^{'x}$ and the equations are spatially averaged over the long AC spatial scale $\xi_i$. $\langle\cdot,\cdot\rangle_x$ represents the spatial average of the short spatial variable $x_i$, the superscript $^{'x}$ represents the fluctuation over the short spatial scale $x$. In 2T-1S, only the time decomposition and averaging is applied. In 1T-2S, only the spatial decomposition and averaging is applied. (v) Physical interpretation of the new equations.

Regardless of the limit used, the above procedure produces a coupled set of LMN and AC equations, as explained in the following subsections.

### 3.2. *Hydrodynamic processes: acoustically forced LMN equations*

Hydrodynamic processes are governed by

$$\frac{\partial\rho}{\partial t} + \nabla^x\cdot(\rho\mathbf{u}) = 0, \tag{3.3}$$

$$\frac{\partial\mathbf{u}}{\partial t} + \mathbf{u}\cdot\nabla^x\mathbf{u} + \frac{1}{\rho}\nabla^x p - \frac{1}{S_1 Re\rho}\nabla^x\cdot\boldsymbol{\tau} = F_{AC\to LMN}, \tag{3.4}$$

$$\nabla^x\cdot\mathbf{u} - \frac{1}{S_1 RePr}\Delta^x T - \rho DaQ_R = 0, \tag{3.5}$$

$$\rho\left[(S_1-1)Z+1\right]\left[(S_2-1)T+1\right] - 1 = 0, \tag{3.6}$$

$$\frac{\partial Z}{\partial t} + \mathbf{u}\cdot\nabla^x Z - \frac{1}{S_1 ReSc\rho}\Delta^x Z = 0, \tag{3.7}$$

where $\nabla^x$ is acting on the hydrodynamic spatial scale, $x_i$. This nonlinear problem can be conveniently expressed in operator matrix-like form as

$$\mathbf{B}\dot{\mathbf{q}}_{LMN} - \mathbf{LMN}(\mathbf{q}_{LMN}) = \mathbf{F}_{AC\to LMN}(\mathbf{q}), \tag{3.8}$$

where $\mathbf{q}_{LMN} = (\rho,\mathbf{u},T,Z,p)^T$ is the vector of the LMN variables; $\dot{\mathbf{q}}_{LMN} = \partial/\partial t\mathbf{q}_{LMN}$; $\mathbf{B}$ the identity matrix with the last row of zeros; $\mathbf{q} = (\mathbf{q}_{LMN},\mathbf{q}_{AC})^T$, with $\mathbf{q}_{AC}$ being the vector of the acoustic variables (see Section 3.3); and the forcing term $\mathbf{F}_{AC\to LMN} = (0,F_{AC\to LMN},0,1,0)^T$. The hydrodynamic operator, $\mathbf{LMN}$, is nonlinear because of the convective derivatives and reaction term.

### 3.3. *Acoustic processes: hydrodynamically forced AC equations*

The AC variables are governed by

$$\frac{\partial\rho^{'\tau}}{\partial\tau} + \nabla^\xi\cdot\left(\langle\rho\rangle_x\,\mathbf{u}^{'\tau}\right) = F_{LMN\to AC_{con}}, \tag{3.9}$$

$$\frac{\partial\mathbf{u}^{'\tau}}{\partial\tau} + \frac{1}{\langle\rho\rangle_x}\nabla^\xi p^{'\tau} = F_{LMN\to AC_{mom}}, \tag{3.10}$$

$$\frac{\partial p^{'\tau}}{\partial\tau} + \nabla^\xi\cdot\mathbf{u}^{'\tau} = F_{LMN\to AC_{en}}. \tag{3.11}$$

where $\nabla^\xi$ acts on the acoustic spatial scale, $\xi_i$. This problem can be expressed as

$$\dot{\mathbf{q}}_{AC} - \mathbf{AC}\mathbf{q}_{AC} = \mathbf{F}_{LMN\to AC}(\mathbf{q}), \tag{3.12}$$

| | 2T-2S | 2T-1S | 1T-2S |
|---|---|---|---|
| $F_{LMN\to AC_{con}}$ | $-\nabla^{\xi}\cdot\left(\langle\rho\rangle_x\left\langle\mathbf{u}'^{\tau}\right\rangle_x+\left\langle\rho'^{x}\mathbf{u}'^{x}\right\rangle_x\right)$ | 0 | $-\nabla^{\xi}\cdot\left(\left\langle\rho'^{x}\mathbf{u}'^{x}\right\rangle_{x'}\right)$ |
| $F_{LMN\to AC_{mom}}$ | 0 | 0 | $-1/\langle\rho\rangle_x\,\partial/\partial t\left\langle\rho'^{x}\mathbf{u}'^{x}\right\rangle_x$ |
| $F_{LMN\to AC_{en}}$ | $-\left\langle\nabla^{\xi}\cdot\mathbf{u}\right\rangle_x$ | $DaQ'^{\tau}_{R0}$ | $Da\,\langle Q_{R1}\rangle_x$ |
| $F_{AC\to LMN}$ | $-1/\rho\nabla^{x}\cdot\left\langle\rho\mathbf{u}'^{\tau}\otimes\mathbf{u}'^{\tau}\right\rangle_\tau$ | $-1/\rho\nabla^{x}\cdot\left\langle\rho\mathbf{u}'^{\tau}\otimes\mathbf{u}'^{\tau}\right\rangle_\tau$ | $-1/\rho\nabla^{\xi}p'^{\tau}$ |

TABLE 1. Terms coupling hydrodynamics to acoustics, $LMN\to AC$, and acoustics to hydrodynamics, $AC\to LMN$. These terms depend on the multiple-scale limit. Double-time-double-space limit is labeled 2T-2S, double-time-single-space labeled 2T-1S, single-time-double-space limit labeled 1T-2S. In 2T-1S $x=\xi$, in 1T-2S $t=\tau$. The numeric subscripts of $Q_{R0}$ and $Q_{R1}$ are the orders of the reaction heat release asymptotic expansion of item $(a)$ in Section 3.1.

where $\mathbf{q}_{AC}=(\rho'^{\tau},\mathbf{u}'^{\tau},p'^{\tau})^T$ is the vector of the AC variables; $\dot{\mathbf{q}}_{AC}=\partial/\partial\tau\mathbf{q}_{AC}$; and the forcing term $\mathbf{F}_{LMN\to AC}=(F_{LMN\to AC_{con}},F_{LMN\to AC_{mom}},F_{LMN\to AC_{en}})^T$. The acoustic operator, **AC**, is linear. Continuity, state, and mixture fraction equations (not shown) are required for calculation of the heat release term in 2T-1S and 1T-2S (Section 3.4).

Physically, the acoustics lose energy by viscous-thermal effects in the boundary layer and by radiation from open ends of the tube. Boundary layer effects would show up as higher order terms because they are globally negligible except in the near-wall region. Ad-hoc damping models need to be implemented. There are two viable routes: modeling the damping as a forcing term in the acoustic equations, or implementing impedance boundary conditions at the combutstor open ends. The first route is more empirical. Route two makes the final eigenvalue problem nonlinear. In this paper, we use the first route, leaving for future work the implementation of the impedance boundary conditions.

### 3.4. *Coupling terms*

The terms coupling the hydrodynamics to the acoustics depend on the multiple-scale limit considered (Table 1). In the double-time-double-space approach (2T-2S in Table 1), the hydrodynamics feeds into the acoustic energy via the (spatial average of) divergence of the hydrodynamic velocity, which is linear. The acoustic velocity feeds into the hydrodynamics via the nonlinear term $-1/\rho\nabla^{x}\cdot\langle\rho\mathbf{u}'^{\tau}\otimes\mathbf{u}'^{\tau}\rangle_\tau$. If the acoustic time scale is larger than the Kolmogorov scale and smaller than the integral scale, this term contains interactions between fluctuations at sub- and resolved scales (Balaji 2012, pp. 45–47). This is seen from $\mathbf{u}'^{\tau}=\langle\mathbf{u}'^{\tau}\rangle_x+\mathbf{u}'^{x'\tau}$, where $\mathbf{u}'^{x'\tau}$ is at unresolved scales. The resolved forcing term, which does not require any closure model, is the acoustic Reynolds stress (ARS) $-1/\rho\nabla^{x}\cdot\langle\rho\langle\mathbf{u}'^{\tau}\rangle_x\otimes\langle\mathbf{u}'^{\tau}\rangle_x\rangle_\tau$ (Lighthill 1978). We neglect sub-grid scale interactions in the acoustics. Also, the acoustic continuity equation is fed by the hydrodynamics.

In the double-time-single-space approach (column 2T-1S of Table 1), the hydrodynamics feeds into the acoustics via the heat release, which is calculated by using the acoustic density, temperature and mixture-fraction equations. As in the 2T-2S limit, the acoustic velocity feeds back into the hydrodynamic momentum via the ARS.

In the single-time-double-space approach (column 1T-2S of Table 1), the hydrodynamics feeds into the acoustics via the fluctuating heat release, as in the 2T-1S limit. The acoustic pressure gradient, which is linear, feeds back into the hydrodynamic momentum. Also, the acoustic continuity and momentum equations are fed by the coupling terms $\sim\langle\rho'^{x}\mathbf{u}'^{x}\rangle_x$, which are the spatial average of the hydrodynamic-spatial (time-averaged) fluctuations, which can be linearized around the mean flow.

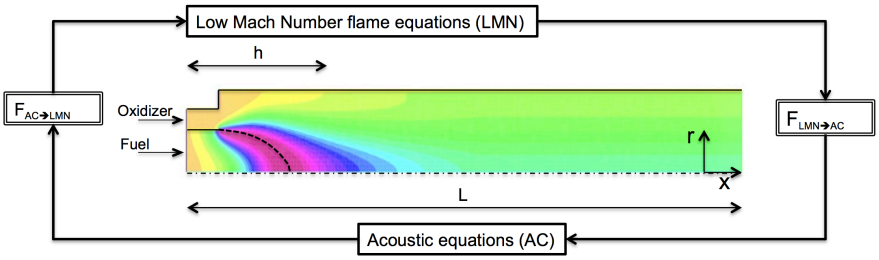


FIGURE 1. Coupling between combusting hydrodynamic (LMN) and acoustic phenomena (AC) via the method of asymptotic multiple scales. Regardless of the multiple-scale limit used, the hydrodynamics feeds into the acoustics, which feed back creating a closed loop. This schematic coupling holds when the Mach number, $M$, is small and the flame length, $h$, is much shorter than the longitudinal hydrodynamic/combustion length, $L$. (As a guide: $M < 0.1$ and $h/L < 0.1$). Depending on the multiple-scale limit, the coupling terms, $F_{AC\to LMN}$ and $F_{LMN\to AC}$, assume different expressions (see Table 1). The image shows the time-averaged temperature of a diffusion-flame dump combustor. The time-average flame front is drawn with a dashed line.

The ARS scales with the acoustic velocity squared, while the acoustic pressure gradient scales with the pressure. Both are linearized around zero, which means that the ARS will play a negligible role in the linear dynamics. Balaji (2012) contains a good summary of these limits.

The coupled thermo-acoustic problem, governed by Eqs. (3.8) and (3.12), is (Figure 1)

$$\mathbf{M}\dot{\mathbf{q}} - \mathbf{TA}\left(\mathbf{q}\right) = \mathbf{F}, \tag{3.13}$$

where $\mathbf{TA}\left(\mathbf{q}\right)$ is the nonlinear thermo-acoustic operator; $\mathbf{M}$ is the concatenation of $\mathbf{B}$ and identity matrices; and $\mathbf{F} = \left(\mathbf{F}_{AC\to LMN}, \mathbf{F}_{LMN\to AC}\right)^T$.

## 4. Linearization

Different multiple-scale limits cause different linear behaviors. In linearization, the LMN variables are split as $\mathrm{LMN} = \mathrm{LMN}_0 + \epsilon\mathrm{LMN}_1 + \alpha\mathrm{LMN}_T$; $\mathrm{LMN}_0 \sim O(1)$ is the steady base flow or time-averaged mean flow; $\epsilon\mathrm{LMN}_1$ is the low-frequency large-scale organized wave with $\epsilon \sim o(1)$; and $\alpha\mathrm{LMN}_T$ the turbulent fluctuation (Reynolds & Hussain 1972). Following Mettot *et al.* (2014), we assume that $\alpha \sim o(\epsilon)$ and neglect the turbulent fluctuations in the linearized problem. Here, $\epsilon \sim o(1)$ denotes the generic amplitude order in linearization, not the perturbation parameter of Section 3. Ideally, $\mathrm{LMN}_0$ should be calculated from DNS or experiments. The linear analysis on time-averaged LES flows works well for predicting low-frequency instabilities, as explained by Mettot *et al.* (2014), on the basis of the theoretical foundations of Reynolds & Hussain (1972). The AC variables are split as $\mathrm{AC} = \mathrm{AC}_0 + \epsilon\mathrm{AC}_1$, $\mathrm{AC}_0 = 0$ is the steady acoustic flow. Therefore, the $\mathrm{LMN}_1$ and $\mathrm{AC}_1$ perturbations fields are of the same order $\epsilon$ but acting at different scales.

When linearized, the thermo-acoustic problem can be expressed in matrix-like form as

$$\mathbf{M}\dot{\mathbf{q}} = \mathbf{J}\mathbf{q}, \tag{4.1}$$

$$\mathbf{J} = \frac{\partial \mathbf{TA}}{\partial \mathbf{q}}\Big|_{(\mathrm{LMN}_0,\mathrm{AC}_0)} = \begin{bmatrix} \left(\frac{\partial \mathbf{LMN}}{\partial \mathbf{q}_{LMN}} + \frac{\partial \mathbf{F}_{AC\to LMN}}{\partial \mathbf{q}_{LMN}}\right) & \frac{\partial \mathbf{F}_{AC\to LMN}}{\partial \mathbf{q}_{AC}} \\ \frac{\partial \mathbf{F}_{LMN\to AC}}{\partial \mathbf{q}_{LMN}} & \left(\mathbf{AC} + \frac{\partial \mathbf{F}_{LMN\to AC}}{\partial \mathbf{q}_{LMN}}\right) \end{bmatrix}_{(\mathrm{LMN}_0,\mathrm{AC}_0)}. \tag{4.2}$$

The Jacobian operator, $\mathbf{J}$, should be viewed as a tensor derivative.

When linearizing the double-time limits 2T-2S and 2T-1S, the ARS, which is the term coupling the acoustics to the LMN, vanishes. The linear dynamics is only one-way coupled because $\delta\mathbf{F}_{AC\to LMN} = o(\epsilon)$ in Eq. (4.2). We may as well solve the LMN linear problem and then feed this into the AC. So, when two time scales are considered, the stability of the one-way coupled problem is governed by the stability of the LMN field. Physically, when there are two time scales (the acoustic time being faster than the convective time), the acoustics are driven by the hydrodynamics but do not affect it. Intuitively, this is because the influence of the acoustics averages out over the long time scale of the hydrodynamics. In a flame transfer function, we see this as a drop in gain at high frequencies (i.e., flames are low-pass filters). Physically, and from this two-scale argument, a thermo-acoustic oscillation requires the time scales to be the same. In a classic picture of a thermo-acoustic instability, the two time scales are indeed the same. On the other hand, when only one time scale is modelled as in 1T-2S, the thermo-acoustic system is two-way coupled because $\delta\mathbf{F}_{AC\to LMN} = O(\epsilon)$. Because most thermo-acoustic problems evolve at different spatial scales and, in good approximation, at the same time scale (Mariappan & Sujith 2011), we infer that there could be a non-trivial interaction between hydrodynamic, acoustic and thermo-acoustic instabilities. The ultimate purpose is to shed light on these interactions by applying sensitivity methods to combustors.

## 5. Sensitivity analysis of the linearized problem

Using the multiple-scale limit 1T-2S, we can set up the eigenproblem of Eq. (4.1), which is $\sigma\mathbf{M}\hat{\mathbf{q}} = \mathbf{J}\hat{\mathbf{q}}$, where $\sigma$ is the complex eigenvalue and $\hat{\mathbf{q}}$ the eigenfunction representing the wavy coherent motion.

The sensitivity of the eigenvalue to mean-flow modifications, $\nabla_{\mathbf{q}_0}\sigma$, is such that the first-order eigenvalue drift is $\delta\sigma = \langle\nabla_{\mathbf{q}_0}, \delta\mathbf{q}_0\rangle$, where $\langle\cdot,\cdot\rangle$ is a non-degenerate bilinear form. The adjoint operators $\mathbf{J}^+$ and $\mathbf{M}^+$ are defined such that, for any arbitrary suitable eigenfunctions $\hat{\mathbf{q}}^+$ and $\hat{\mathbf{q}}$, the duality pairing $\langle\hat{\mathbf{q}}^+, (\sigma\mathbf{M} - \mathbf{J})\hat{\mathbf{q}}\rangle = \langle(\sigma^+\mathbf{M}^+ - \mathbf{J}^+)\hat{\mathbf{q}}^+, \hat{\mathbf{q}}\rangle$ holds. The adjoint modes $\hat{\mathbf{q}}^+$ are the eigenfunctions of the adjoint eigenproblem $\sigma^+\mathbf{M}^+\hat{\mathbf{q}}^+ = \mathbf{J}^+\hat{\mathbf{q}}^+$. Note that $\sigma^+{=}\sigma^*$, $\mathbf{M}^+ = \mathbf{M}^{T*}$, and $\mathbf{J}^+ = \mathbf{J}^{T*}$, $*$ being the complex conjugation, when the bilinear form is a Hermitian inner product. The eigenvalue sensitivity is conveniently calculated with a combination of the direct and adjoint modes, $\nabla_{\mathbf{q}_0}\sigma = \mathbf{H}^+\hat{\mathbf{q}}^+$, where $\mathbf{H} = \partial\left(\mathbf{J}\hat{\mathbf{q}}\right)/\partial\mathbf{q}_0$ is the Hessian applied to the global mode $\hat{\mathbf{q}}$. We assume that the linearized eddy-viscosity is zero (quasi-laminar assumption), i.e., the linearized operator, $\mathbf{J}$, has only molecular viscosity. The eigenvalue drift owing to a steady passive forcing is $\delta\sigma = \langle\nabla_{\mathbf{f}}\sigma, \delta\mathbf{f}\rangle$ with $\nabla_{\mathbf{f}}\sigma = \left(\mathbf{J}^+\right)^{-1}\nabla_{\mathbf{q}_0}\sigma$. The imaginary part of $\nabla_{\mathbf{f}}\sigma$ provides the spatial sensitivity map for a feedback device to change the large-scale wave frequency. For more details, the reader may refer to Mettot *et al.* (2014).

## 6. Preliminary results

The space is discretised using finite bubble elements (www.freefem.org/ff++/) which are more stable than Taylor-Hood elements in combusting problems. Matrix inversions

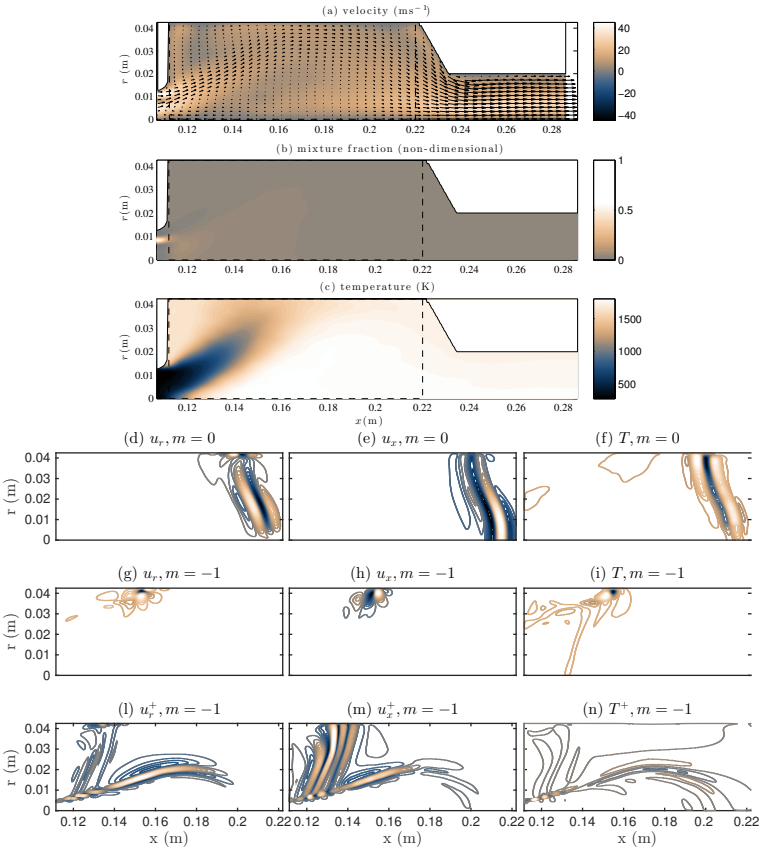


FIGURE 2. Base flow and first global modes in the dual-swirl combustor. The bottom horizontal line denotes the centerline. First row: velocity; second row: mixture fraction; third row: temperature. The dashed box marks the border of the displayed global mode results. Fourth row: m=0 direct eigenfunction, which is convectively unstable; fifth row: m=-1 direct eigenfunction, which is absolutely unstable; sixth row: m=-1 adjoint eigenfunction, showing the area of highest receptivity to open loop forcing. Positive values in light color, negative values in dark. The eigenfunctions are non-dimensional.

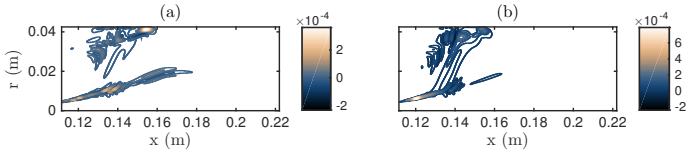


FIGURE 3. Imaginary part of the sensitivity to mean-flow modifications to (a) radial velocity, (b) axial velocity in non-dimensional units.

are performed with MUMPS, a highly parallel algorithm (mumps.enseeiht.fr/). The eigenproblem is solved by a shift-invert method with ARPACK (www.caam.rice.edu/software/ARPACK/). The problem is solved in cylindrical coordinates and the variables are Fourier-transformed in the azimuthal direction as $\phi(r, x, \theta) \rightarrow \phi(r, x) \exp(m\theta)$, in which $\phi$ is a generic variable.

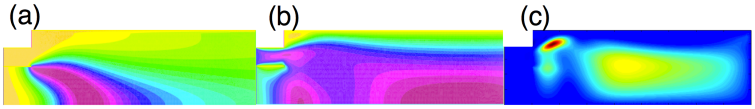


FIGURE 4. Simplified dump combustor geometry. The bottom horizontal line denotes the centerline. The fields are (a) mean-flow temperature (light color=min=0; dark color=max$\approx$ 0.8); (b) mean-flow axial velocity (light color=min=0; dark color=max$\approx$ 3); (c) absolute value of the highest eigenvalue sensitivity component (radial).

### 6.1. *Hydrodynamic analysis of the dual-swirl combustor*

The case presented has $Re = 47000$ (turbulent flow) and standard air properties. Results of the hydrodynamic analysis are reported in Figures 2 and 3. Acoustic analysis and thermo-acoustic coupling is underway.

The mean flow is obtained by time averaging the LES simulation obtained with CharLES (See & Ihme 2014) (top three panels in Figure 2). Although the flow is not completely axisymmetric, we assume axisymmetry and study a slice, which has been symmetrized and smoothed. The flow is partially premixed, meaning that both mixture fraction and progress variables are in the state vector of the LES simulation. In the linearized analysis, we model the mixture fraction only, leaving the consideration of the progress variable for future work. The axisymmetric mode $m = 0$ is convectively unstable but globally stable (Figure 2(a-c)). The flow is globally unstable to the $m = -1$ helical mode (Figure 2(d-f)). The angular frequency of this mode is $\approx 5000\ rad/s$. The greatest receptivity is localized along the flame (Figure 2(g-i)). Open loop forcing is most efficient there but this could be an impractical control strategy. The highest sensitivity to feedback mechanisms is where the flow impinges on the wall. The most efficient mechanism should react to the radial velocity and act on the radial momentum equation (Figure 3(a)). The maps in Figure 3 also suggest how to modify the inlet velocity profile to reduce the frequency of the coherent large-scale motion. For example, decreasing the radial component at the flame base would lower the coherent-motion frequency (Figure 3(b)).

### 6.2. *Combusting hydrodynamic analysis of a dump combustor*

The case presented has the following parameters: $Re = 100$ (laminar flow); $Pr = Sc = 0.7$; $\kappa = 0.01$; $s = 2$; $\beta = 3$; $S_1 = 7$; $S_2 = 6$; $Da = 10^6$. Results are reported in Figure 4. The flow is globally stable. The mean flow is obtained by time averaging the simulation obtained with a structured finite-volume based LES solver. The flow is governed by the equations reported in this paper. The highest sensitivity to feedback mechanisms straddle the recirculation bubble. This means that the active feedback mechanism is mostly the result of non-reacting hydrodynamic phenomena. Thermo-acoustic coupling is underway.

## 7. Discussion and outlook

In summary, we have derived general equations for 3D thermo-acoustic systems in low-Mach number combustors. We used an asymptotic method and discussed three multiple scale limits. Only the single-time-double-space limit allows the linearized dynamics to be two-way coupled. Using this limit, we defined an eigenproblem and showed how to study the sensitivity conveniently with adjoint eigenfunctions. We showed preliminary results on two combustors. The full numerical thermo-acoustic coupling is underway.

*Acknowledgments*

The authors acknowledge use of computational resources from the Certainty cluster awarded by the National Science Foundation to the CTR. L.M. is grateful to Dr. O. Tammisola, Dr. V. Citro, Dr. U. Qadri, C. Hennekinne, Dr. C. Balaji and Prof. S.R. Chakravarthy for insightful discussions. This work is supported by the 2014 CTR Summer Program and the European Research Council - Project ALORS 2590620.

## REFERENCES

Allison, P. M., Driscoll, J. F. & Ihme, M. 2013 Acoustic characterization of a partially-premixed gas turbine model combustor: Syngas and hydrocarbon fuel comparisons. *Proc. Combus. Inst.* **34**, 3145–3153.

Balaji, C. 2012 *Investigation of flame-acoustic coupling in a backward-facing step combustor*. PhD thesis, IIT Madras.

Chakravarthy, S. R., Shreenivasan, O. J., Boehm, B., Dreizler, A. & Janicka, J. 2007 Experimental characterization of onset of acoustic instability in a nonpremixed half-dump combustor. *J. Acoust. Soc. Am.* **122**, 120–127.

Giezendanner, R., Weigand, P., Duan, X. R., Meier, W., Meier, U., Aigner, M. & Lehmann, B. 2005 Laser-Based Investigations of Periodic Combustion Instabilities in a Gas Turbine Model Combustor. *J. Eng. Gas Turb. Power* **127**, 492–496.

Klein, R. 2005 Multiple spatial scales in engineering and atmospheric low Mach number flows. *Math. Model. Num.* **39**, 537–559.

Lighthill, J. 1978 Acoustic streaming. *J. Sound Vib.* **61**, 391–418.

Mariappan, S. & Sujith, R. I. 2011 Modelling nonlinear thermoacoustic instability in an electrically heated Rijke tube. *J. Fluid Mech.* **680**, 511–533.

Mettot, C., Sipp, D. & Bézard, H. 2014 Quasi-laminar stability and sensitivity analyses for turbulent flows: Prediction of low-frequency unsteadiness and passive control. *Phys. Fluids* **26**, 045112.

Müller, B. 1998 Low-Mach-number asymptotics of the Navier-Stokes equations. *J. Eng. Math.* **34**, 97–109.

Nichols, J. W. & Schmid, P. J. 2008 The effect of a lifted flame on the stability of round fuel jets. *J. Fluid Mech.* **609**, 275–284.

Reynolds, W. C. & Hussain, K. M. F. 1972 The mechanics of an organized wave in turbulent shear flow. Part 3. Theoretical models and comparisons with experiments. *J. Fluid Mech.* **54**, 263–288.

See, Y. C. & Ihme, M. 2014 Large eddy simulation of a partially-premixed gas turbine model combustor. *Proc. Combus. Inst.,* In Press.

Zeytounian, R. K. 2006 *Topics in Hyposonic Flow Theory*. Springer-Verlag.